

Determination of the $K^+\bar{K}^0$ scattering length and effective range from the $D^+ \rightarrow \bar{K}^0\pi^+\eta$ reaction

Jing Song,^{1,2} Wei-Hong Liang,^{3,4,*} and Eulogio Oset^{2,3,†}

¹*School of Physics, Beihang University, Beijing, 102206, China*

²*Departamento de Física Teórica and IFIC, Centro Mixto Universidad de Valencia-CSIC Institutos de Investigación de Paterna, 46071 Valencia, Spain*

³*Department of Physics, Guangxi Normal University, Guilin 541004, China*

⁴*Guangxi Key Laboratory of Nuclear Physics and Technology, Guangxi Normal University, Guilin 541004, China*

We study the scattering parameters of the $K^+\bar{K}^0$ system through the analysis of the $D^+ \rightarrow \bar{K}^0\pi^+\eta$ reaction, aiming at determining the scattering length a and effective range r_0 of the $K^+\bar{K}^0$ interaction. These parameters are extracted by analyzing and fitting the mass distributions of the pairs in the final $\bar{K}^0\pi^+\eta$ state. To ensure the reliability of the results, we apply resampling techniques to evaluate statistical uncertainties and improve the precision of the scattering parameters. The obtained results are compared with previous theoretical predictions and experimental data, providing new insights into the $K^+\bar{K}^0$ interaction at low energies.

I. INTRODUCTION

The decay process $D^+ \rightarrow K_s^0\pi^+\eta$ has been studied by the BESIII collaboration, first in Ref. [1] and later with higher precision and an amplitude analysis in Ref. [2]. This process is useful for studying the $a_0(980)$ resonance, which is an important scalar meson. The actual reaction is $D^+ \rightarrow \bar{K}^0\pi^+\eta$, where the \bar{K}^0 is detected as a K_s^0 state. In Ref. [3], the theoretical analysis of the $D^+ \rightarrow \bar{K}^0\pi^+\eta$ reaction was studied to understand the nature of the $a_0(980)$ in this reaction. The authors found that the $a_0(980)$ production is the dominant term in this reaction and also discussed other terms that interfere with this production mode.

Initially, as mentioned in Ref. [3], this reaction is similar to the $D^0 \rightarrow K^-\pi^+\eta$ decay studied by Belle [4], as the latter can be obtained by replacing a \bar{d} quark with a \bar{u} quark. However, there are notable differences. In the $D^0 \rightarrow K^-\pi^+\eta$ decay, the $K^-\pi^+$ system is dominated by the \bar{K}^{*0} resonance, creating a strong peak. In contrast, in the $D^+ \rightarrow \bar{K}^0\pi^+\eta$ decay, the $\bar{K}^0\pi^+$ system cannot originate from \bar{K}^{*0} or K^{*-} , resulting in the absence of the \bar{K}^* contribution. This absence makes the process a good tool to study the $a_0(980)$ resonance independently [2].

The theoretical analysis of the $D^0 \rightarrow K^-\pi^+\eta$ reaction was studied in Ref. [5]. It found that the $K^-\pi^+$ mass distribution has a sharp peak at the \bar{K}^{*0} threshold, while the $\pi^+\eta$ mass distribution contains significant contributions of low and high invariant masses because of the \bar{K}^{*0} resonance. The $K^-\eta$ mass distribution also displays a double peak from the \bar{K}^{*0} . On the other hand, in $D^+ \rightarrow \bar{K}^0\pi^+\eta$, the $\bar{K}^0\pi^+$ mass distribution has no sharp structures, and the $\pi^+\eta$ distribution is dominated by the $a_0(980)$ resonance, which makes it easier to study this scalar meson. The $\bar{K}^0\eta$ mass distribution also shows a significantly different behavior.

Studying the weak decays of heavy mesons is essential for understanding hadron interactions and dynamically generated states. Three-body decays are particularly useful to explore hadronic final-state interactions and study the resonance nature of states [6–8]. The $D^+ \rightarrow \bar{K}^0\pi^+\eta$ reaction, which was recently measured with high precision [2], provides an opportunity to investigate the $a_0(980)$ resonance and extract the $K^+\bar{K}^0$ scattering parameters with minimal background interference from other factors.

The $a_0(980)$ is known to strongly couple to the $K\bar{K}$ channel and has been studied in various reactions [6, 7, 9, 10]. However, it is difficult to determine the $K^+\bar{K}^0$ scattering length and effective range because of the complexity of final-state interactions and coupled-channel effects [11–15]. Sometimes, these parameters can be obtained from cusp structures in invariant mass distributions. This method has been successfully applied to the $\pi^+\pi^-$ system in $K \rightarrow 3\pi$ decays [16, 17] and more recently to the $\Lambda_c^+ \rightarrow pK^-\pi^+$ decay [18], which allowed a precise measurement of the $\eta\Lambda$ scattering length [19].

In this work, following the study of Ref. [3], we focus on the $D^+ \rightarrow \bar{K}^0\pi^+\eta$ reaction using a coupled-channel unitary approach [6, 7] to determine the $K^+\bar{K}^0$ scattering parameters. This approach has been successfully applied to studies of dynamically generated scalar mesons [20, 21]. To get an accurate determination of the scattering parameters and their errors, we apply a statistical resampling method [22], which helps to measure uncertainties in fits to the experimental data.

Previous experimental studies have provided estimates of the $K^+\bar{K}^0$ scattering length, but the results differ quite a bit [11–15]. The high-statistics measurement by BESIII [2] provide a unique opportunity to refine these values and improve our understanding of the strong interaction dynamics in the scalar sector. The results from this study will not only improve knowledge about the

*liangwh@gxnu.edu.cn

†oset@ific.uv.es

$a_0(980)$ resonance but also provide crucial input for future research on scalar mesons and their role in hadron spectroscopy [23–25].

II. FORMALISM

We study the $D^+ \rightarrow \bar{K}^0 \pi^+ \eta$ reaction and look at the mechanisms for external and internal emission based on the same formalism in Ref. [3], except for the external emission process.

A. External emission

In Fig. 1 we show the mechanism of external emission, Cabibbo favoured, at the quark level, and in Fig. 2 we show the hadronization of quark pairs into two mesons.

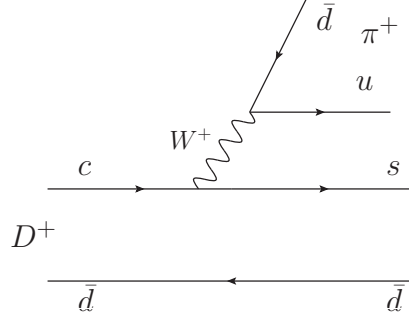


FIG. 1: Mechanism with external emission at the quark level.

In Fig. 2 (a), the $s\bar{d}$ pair is hadronized in the following way:

$$s\bar{d} \rightarrow \sum_i s \bar{q}_i q_i \bar{d}, \quad (1)$$

which is easily interpreted writing the $q_i \bar{q}_j$ matrix in terms of pseudoscalar mesons, \mathcal{P}_{ij} , which in the standard $\eta - \eta'$ mixing of Ref. [26] is given by

$$\mathcal{P} = \begin{pmatrix} \frac{1}{\sqrt{2}}\pi^0 + \frac{1}{\sqrt{3}}\eta & \pi^+ & K^+ \\ \pi^- & -\frac{1}{\sqrt{2}}\pi^0 + \frac{1}{\sqrt{3}}\eta & K^0 \\ K^- & \bar{K}^0 & -\frac{1}{\sqrt{3}}\eta \end{pmatrix}. \quad (2)$$

Hence,

$$s\bar{d} \rightarrow \sum_i \mathcal{P}_{3i} \mathcal{P}_{i2} = (\mathcal{P}^2)_{32} = K^- \pi^+ - \bar{K}^0 \frac{\pi^0}{\sqrt{2}}, \quad (3)$$

where the $\bar{K}^0 \eta$ component has canceled.

The combination of Eq. (3), together with the π^+ of Fig. 1, does not lead to the desired final state $\bar{K}^0 \pi^+ \eta$. However, through rescattering the $K^- \pi^+$ and $\bar{K}^0 \pi^0$ could lead to $\bar{K}^0 \eta$. Yet, the threshold of $\bar{K}^0 \eta$ is 1040 MeV, which is about 300 MeV above the peak of the $K_0^*(700)$ (the kappa), where the $K^- \pi^+ \rightarrow \bar{K}^0 \eta$ amplitude has a reduced strength, and because of that we shall disregard this contribution, as it was also done in Ref. [5].

Next, with the same mechanism of Fig. 1, we look at the hadronization of the $\bar{d}u$ component, as shown in Fig. 2(b).

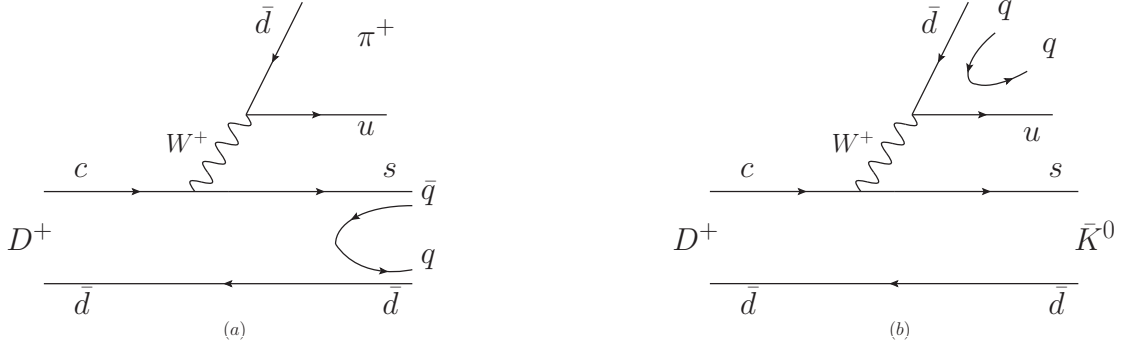


FIG. 2: Hadronization of the $s\bar{d}$ (a), and hadronization of the $u\bar{d}$ (b) component in external emission.

We have now

$$u\bar{d} \rightarrow \sum_i u \bar{q}_i q_i \bar{d} = \sum_i \mathcal{P}_{1i} \mathcal{P}_{i2} = (\mathcal{P}^2)_{12}. \quad (4)$$

Hence we have now the combination

$$H = \left(\frac{\pi^0}{\sqrt{2}} + \frac{\eta}{\sqrt{3}}\right)\pi^+ + \pi^+ \left(-\frac{\pi^0}{\sqrt{2}} + \frac{\eta}{\sqrt{3}}\right) + K^+ \bar{K}^0. \quad (5)$$

It might look like the two terms with $\eta\pi^+$ add and the two terms with $\pi^+\pi^0$ cancel. However, this is not the case as we show below. This is something peculiar of the external emission, when the W^μ couples directly to two mesons. Indeed, as done in the Ref. [27], one starts with the Langrangian of WPP [28, 29],

$$\mathcal{L} = \frac{f^2}{4} \langle D_\mu U (D^\mu U)^\dagger \rangle + \frac{f^2}{4} \langle \chi U^\dagger + U \chi^\dagger \rangle, \quad (6)$$

where

$$\begin{aligned} D_\mu U &= \partial_\mu U - i r_\mu U + i U l_\mu, \\ U &= \exp(i \frac{\sqrt{2} P}{f}), \end{aligned} \quad (7)$$

with r_μ , l_μ the right-handed, left-handed weak interaction currents

$$\begin{aligned} r_\mu &= v_\mu + a_\mu = e Q A_\mu + \dots, \\ l_\mu &= v_\mu - a_\mu = e Q A_\mu + \frac{e}{\sqrt{2} \sin \theta_W} (W_\mu^\dagger T_+ + W_\mu T_-), \end{aligned} \quad (8)$$

where

$$T_+ = \begin{pmatrix} 0 & V_{ud} & V_{us} \\ 0 & 0 & 0 \\ 0 & 0 & 0 \end{pmatrix}, \quad T_- = \begin{pmatrix} 0 & 0 & 0 \\ V_{ud} & 0 & 0 \\ V_{us} & 0 & 0 \end{pmatrix}, \quad (9)$$

with V_{ud} , V_{us} , matrix elements of the Cabibbo–Kobayashi–Maskawa matrix. Where, v_μ , a_μ , A_μ , and W_μ are the vector current, axial current, electro magnetic field, and W field, q the electron charge and Q the matrix of the charge of quarks u , d , s . We are only concerned on the weak part of l_μ . After expansion of the fields, one finds for the $W P_1 P_2$ vertex of Fig. 2 (b)

$$\mathcal{L} = -i \frac{1}{2} \frac{e}{\sqrt{2} \sin \theta_W} W_\mu^+ \langle [P, \partial_\mu P] T_+ \rangle. \quad (10)$$

What matters for us here is the structure of the term $\langle [P, \partial_\mu P] W^\mu \rangle$. Indeed, if we have $\eta\pi^+$ and $\pi^+\eta$ terms, then we get

$$\begin{aligned} \eta \partial_\mu \pi^+ - \pi^+ \partial_\mu \eta, & \quad \text{from the } \eta\pi^+ \text{ term;} \\ \pi^+ \partial_\mu \eta - \eta \partial_\mu \pi^+, & \quad \text{from the } \pi^+\eta \text{ term,} \end{aligned} \quad (11)$$

and they cancel exactly. By the contrary, the terms $\pi^0\pi^+$ and $\pi^+\pi^0$ of Eq. (5) add, but they do not contribute to the process. The term $K^+\bar{K}^0$ of Eq. (5) could contribute through $K^+\bar{K}^0 \rightarrow \pi^+\eta$, but the structure of Eq. (10), $K^+\partial_\mu\bar{K}^0 - \bar{K}^0\partial_\mu K^+$, with the dominant $\mu = 0$ component, also makes this term vanish in an average through the calculation of the difference of the \bar{K}^0 and K^+ energies. In conclusion, we have found that there is no contribution to the process from external emission¹.

B. Internal Emission

For internal emission, we use the same formalism of Ref. [3], and we show the same formula here for completeness. We utilize the diagrams in Fig. 3, which depict the hadronization of quark pairs.

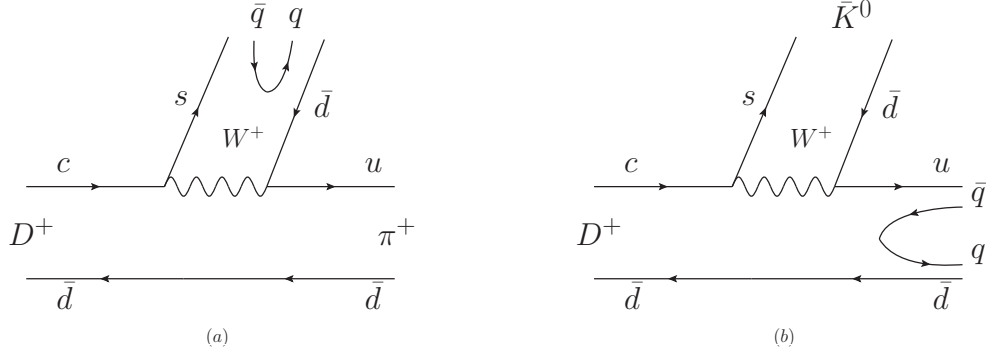


FIG. 3: Diagrams representing internal emission: (a) hadronization of the $s\bar{d}$ pair; (b) hadronization of the $u\bar{d}$ pair.

Following the process outlined in subsection II A, we now describe the hadronization:

$$s\bar{d} \rightarrow \sum_i s \bar{q}_i q_i \bar{d} = \sum_i \mathcal{P}_{3i} \mathcal{P}_{i2} = (\mathcal{P}^2)_{32} = K^-\pi^+ - \frac{1}{\sqrt{2}} \bar{K}^0\pi^0, \quad (12)$$

where the $\bar{K}^0\eta$ terms cancel, and

$$u\bar{d} \rightarrow \sum_i u \bar{q}_i q_i \bar{d} = \sum_i \mathcal{P}_{1i} \mathcal{P}_{i2} = (\mathcal{P}^2)_{12} = \frac{2}{\sqrt{3}} \eta\pi^+ + K^+\bar{K}^0, \quad (13)$$

where the $\pi^+\pi^0$ terms cancel.

Summing the two terms, including the π^+ from Fig. 3 (a) and \bar{K}^0 from Fig. 3 (b), we obtain:

$$H' = K^-\pi^+\pi^+ - \frac{1}{\sqrt{2}} \pi^0\pi^+\bar{K}^0 + \frac{2}{\sqrt{3}} \eta\pi^+\bar{K}^0 + K^+\bar{K}^0\bar{K}^0. \quad (14)$$

Once again we have a tree-level production of $\eta\pi^+\bar{K}^0$, with the other terms potentially leading to this final state via rescattering, as shown in Fig. 4.

¹ We have carried out this detailed discussion, because in our previous paper of Ref. [3] this important fact was not realized, and there was a contribution to the mass distribution from external emission. Yet, the fit to the data demanded a contribution from external emission much smaller than from internal emission. The discussion done here, while supporting the numerical results of [3], justifies this unusual conclusion in Ref. [3]. We take advantage to mention that the V_{23} element of Eq. (17) in [3] should have an opposite sign. It is a typo and the right formula was used in the results.

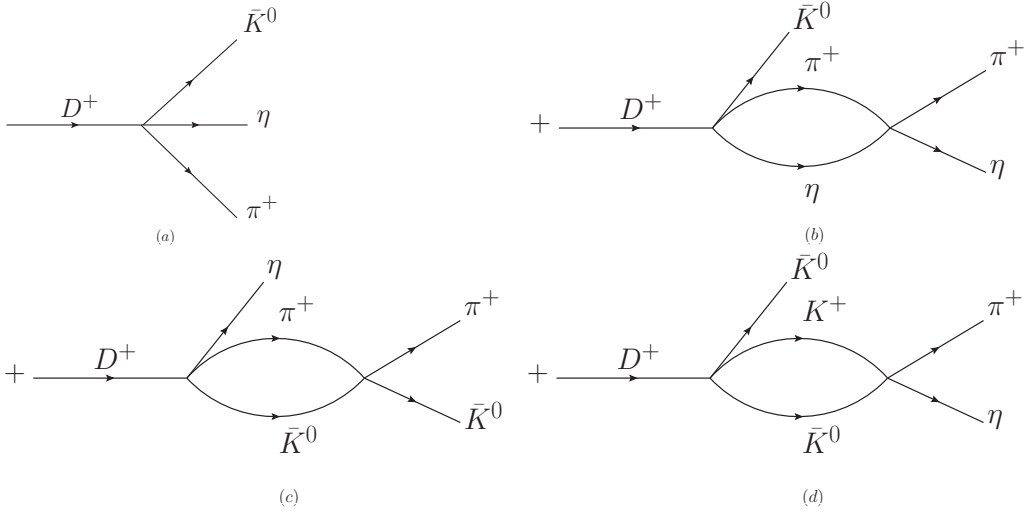


FIG. 4: Diagrams showing the production of $\eta\pi^+\bar{K}^0$ from internal emission: (a) tree level; (b) $\pi^+\eta$ rescattering; (c) $\pi^+\bar{K}^0$ rescattering; (d) $K^+\bar{K}^0$ rescattering.

In Fig. 4, we have ignored possible rescattering processes such as $K^-\pi^+ \rightarrow \bar{K}^0\eta$, $\bar{K}^0\pi^0 \rightarrow \bar{K}^0\eta$, and $\bar{K}^0\eta \rightarrow \bar{K}^0\eta$, for the same reasons discussed in the previous subsection. Numerical checks confirm that these terms are negligible.

We analytically describe the diagrams of Fig. 4 corresponding to internal emission as:

$$t^{(ie)} = \mathcal{C} \left\{ h_{\eta\pi^+\bar{K}^0} \left[1 + G_{\pi^+\eta} \left(M_{\text{inv}}(\pi^+\eta) \right) t_{\pi^+\eta,\pi^+\eta} \left(M_{\text{inv}}(\pi^+\eta) \right) + G_{\pi^+\bar{K}^0} \left(M_{\text{inv}}(\pi^+\bar{K}^0) \right) t_{\pi^+\bar{K}^0,\pi^+\bar{K}^0} \left(M_{\text{inv}}(\pi^+\bar{K}^0) \right) \right] \right. \\ \left. + 2h_{K^+\bar{K}^0\bar{K}^0} G_{K^+\bar{K}^0} \left(M_{\text{inv}}(\pi^+\eta) \right) t_{K^+\bar{K}^0,\pi^+\eta} \left(M_{\text{inv}}(\pi^+\eta) \right) \right\}, \quad (15)$$

where the weights h_i are given by:

$$h_{\eta\pi^+\bar{K}^0} = \frac{2}{\sqrt{3}}; \quad h_{K^+\bar{K}^0\bar{K}^0} = 1, \quad (16)$$

and \mathcal{C} is a global normalization factor to be fitted to the normalization of the data. The factor of 2 multiplying $h_{K^+\bar{K}^0\bar{K}^0}$ in Eq. (15) accounts for the two identical \bar{K}^0 particles.

C. $K_0^*(1430)$ Contribution

We follow the same formula of Ref. [3] to consider the $K_0^*(1430)$ resonance, where the important role of $K_0^*(1430)$ was discussed. In Ref. [2], it was observed that the scalar $K_0^*(1430)$ [$I(J^P) = \frac{1}{2}(0^+)$] state contributes to the $D^+ \rightarrow \bar{K}^0\pi^+\eta$ process and appears in the $K\eta$ mass distribution. The process is depicted in Fig. 5 (we label the particles as \bar{K}^0 (1), π^+ (2), η (3)).

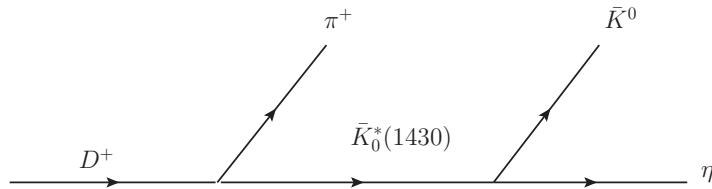


FIG. 5: Diagram representing the process $D^+ \rightarrow \pi^+\bar{K}_0^*(1430) \rightarrow \pi^+\bar{K}^0\eta$.

We account for this contribution phenomenologically by introducing the amplitude:

$$t^* = \mathcal{D} e^{i\phi} \frac{M_D^2}{s_{13} - M_{K_0^*}^2 + i M_{K_0^*} \Gamma_{K_0^*}}, \quad (17)$$

where \mathcal{D} and ϕ are free parameters, and $s_{13} = (p_{\bar{K}^0} + p_\eta)^2$ represents the invariant mass of the \bar{K}^0 and η particles. The factor M_D^2 is included to make \mathcal{D} dimensionless. We take the mass and width from the PDG [30] as $M_{K_0^*} = 1425$ MeV, $\Gamma_{K_0^*} = 270$ MeV.

The total amplitude now becomes:

$$t = t^{(ie)} + t^*. \quad (18)$$

To calculate the mass distributions, we use the standard PDG formula [30]:

$$\frac{d^2\Gamma}{ds_{12} ds_{23}} = \frac{1}{(2\pi)^3} \frac{1}{32 M_D^3} |t|^2. \quad (19)$$

By using the limits of the PDG formula [30], we can obtain $d\Gamma/ds_{12}$ by integrating over s_{23} . Using cyclical permutations of the formulas, we can derive $d\Gamma/ds_{13}$ and $d\Gamma/ds_{23}$ and compare with experimental data [2].

D. Scattering Amplitudes

We need the following amplitudes:

$$t_{\eta\pi^+, \eta\pi^+}, \quad t_{\bar{K}^0\pi^+, \bar{K}^0\pi^+}, \quad t_{\bar{K}^0K^+, \pi^+\eta}.$$

Using the results from Ref. [31] (Eq. (A.4) of Ref. [31]), which explicitly considers $\eta - \eta'$ mixing, we find the matrix elements of the potential for the channels $K^+K^-(1)$, $K^0\bar{K}^0(2)$, $\pi^0\eta(3)$:

$$\begin{aligned} V_{11} &= -\frac{s}{2f^2}, & V_{12} &= -\frac{s}{4f^2}, \\ V_{13} &= -\frac{3s - 2m_K^2 - m_\eta^2}{3\sqrt{6}f^2}, & V_{22} &= -\frac{s}{2f^2}, \\ V_{23} &= \frac{3s - 2m_K^2 - m_\eta^2}{3\sqrt{6}f^2}, & V_{33} &= -\frac{2m_\pi^2}{3f^2}. \end{aligned} \quad (20)$$

Then, the amplitudes t are obtained from the Bethe-Salpeter equation in coupled channels:

$$T = [1 - VG]^{-1} V. \quad (21)$$

Considering that $|\pi^+\rangle = -|11\rangle$ of isospin, we find

$$t_{\eta\pi^+, \eta\pi^+} = t_{\eta\pi^0, \eta\pi^0}. \quad (22)$$

Also, taking into account that K^+K^- in terms of $|I, I_3\rangle$ is:

$$K^+K^- = -\left(\frac{1}{\sqrt{2}}|00\rangle + \frac{1}{\sqrt{2}}|10\rangle\right), \quad (23)$$

then we obtain the $\bar{K}^0K^+ \rightarrow \pi^+\eta$ amplitudes

$$t_{\bar{K}^0K^+, \pi^+\eta} = \sqrt{2} t_{K^+K^-, \pi^0\eta}. \quad (24)$$

We also require the $K\pi \rightarrow K\pi$ amplitudes, which we extract from the Appendix of Ref. [5], considering the channels $\pi^-K^+(1)$, $\pi^0K^0(2)$, and $\eta K^0(3)$. By applying isospin coefficients and the C -parity relation $C\bar{K}^0\pi^+ = K^0\pi^-$, we obtain

$$t_{\bar{K}^0\pi^+, \bar{K}^0\pi^+} = \frac{2}{3}T_{22} + \frac{1}{3}T_{11} + \frac{2\sqrt{2}}{3}T_{12}. \quad (25)$$

And the loop function G_l in Eq. (15) is given by:

$$G_l(\sqrt{s}) = \int_{|q| < q_{\max}} \frac{d^3q}{(2\pi)^3} \frac{(w_1(q) + w_2(q))}{2w_1(q)w_2(q)} \frac{1}{s - (w_1(q) + w_2(q))^2 + i\epsilon}, \quad (26)$$

where $w_i(q) = \sqrt{m_i^2 + \vec{q}^2}$, $i = 1, 2$, with 1, 2 referring to the two particles of channel l . The cutoff is $q_{\max} = 630$ MeV [31].

E. Determination of a and r_0 for $K^+ \bar{K}^0$

The scattering length a and effective range r_0 are given in Ref. [32],

$$\begin{aligned} -\frac{1}{a} &= -8\pi\sqrt{s}T^{-1}\Big|_{s=s_{\text{th}}}, \\ r_0 &= \frac{\sqrt{s}}{\mu} \frac{\partial}{\partial s} 2(-8\pi\sqrt{s}T^{-1} + ik) \Big|_{s=s_{\text{th}}}, \\ k &= \frac{\lambda^{1/2}(s, m_{K^+}^2, m_{\bar{K}^0}^2)}{2\sqrt{s}}, \end{aligned} \quad (27)$$

where T stands for the $T_{K^+ \bar{K}^0, K^+ \bar{K}^0}$ scattering amplitude, s_{th} is the squared energy of the $K^+ \bar{K}^0$ system at threshold, and μ is the reduced mass of K^+ and \bar{K}^0 . To evaluate a and r_0 for $K^+ \bar{K}^0$, one must have very precise values for the thresholds. Since we only need $I = 1$ in this case, we can directly use the $K^+ \bar{K}^0$ and $\pi^+ \eta$ channels.

The V -matrix for the coupled channels $K^+ \bar{K}^0$ and $\pi^+ \eta$ is given by

$$\begin{aligned} V_{11} &= -\frac{s}{4f^2}, \quad V_{12} = -\frac{3s - m_{K^+}^2 - m_{\bar{K}^0}^2 - m_\eta^2}{3\sqrt{3}f^2}, \\ V_{22} &= -\frac{2m_\pi^2}{3f^2}, \end{aligned} \quad (28)$$

with $f = 93$ MeV. The T matrices are then obtained using the Bethe-Salpeter equation in Eq. (21).

III. RESULTS

A. Mass distributions of $\bar{K}^0 \pi^+$, $\bar{K}^0 \eta$, and $\pi^+ \eta$

Our theoretical model involves 3 parameters: \mathcal{C} , \mathcal{D} , and ϕ . To determine their values, we perform a best fit to the mass distributions of $\bar{K}^0 \pi^+$, $\bar{K}^0 \eta$, and $\pi^+ \eta$ using the experimental data from Ref. [2]. The resulting parameter values are listed in Table I.

TABLE I: The value of the parameters \mathcal{C} , \mathcal{D} , and ϕ [radians] from the best fit.

| \mathcal{C} | \mathcal{D} | ϕ [radians] |
|---------------|---------------|------------------|
| 592.48 | 51.328 | -1.747 |

The parameter \mathcal{C} serves as an overall normalization factor. The parameter \mathcal{D} determines the strength of the $K_0^*(1430)$ contribution. Moreover, the phase $\exp(i\phi)$ accounts for the interference between the $K_0^*(1430)$ and other components, playing a important role in shaping the mass distributions.

Figure 6 presents the mass distribution results obtained with the fitted parameters from Table I. A comparison with the experimental data shows that our theoretical predictions accurately describe well the observed distributions.

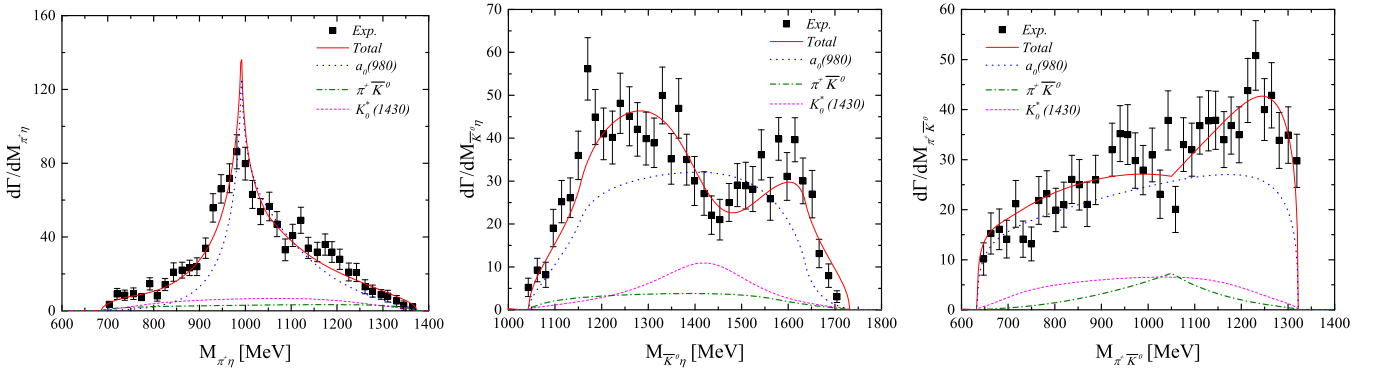


FIG. 6: The mass distributions of $\pi^+\eta$ (left), $\bar{K}^0\eta$ (middle), and $\bar{K}^0\pi^+$ (right) with fixed $M_{\text{cut}} = 1050$ MeV. The parameters $C = 592.48$, $D = 51.328$, and $\phi = -1.747$ radians are used.

We found that the features of the results obtained here in the revised formalism are the same as those in Ref. [3], which were discussed in detail in Ref. [3]. We recall the main features here. In Fig. 6 (left), a pronounced peak appears in the $\pi^+\eta$ spectrum around 1.0 GeV, corresponding to the $a_0(980)$ resonance. In our model, this resonance is encoded in the T -matrix elements $t_{\eta\pi^+, \eta\pi^+}$ and $t_{\bar{K}^0K^+, \eta\pi^+}$, as defined in Eqs. (22) and (24). On the other hand, the contribution from the $\bar{K}^0\pi^+$ scattering term in Eq. (25) and the $K_0^*(1430)$ component is significantly smaller than that of the $a_0(980)$ resonance. It is also important to emphasize that the interference with other components, particularly the tree-level contributions in Eqs. (15), leads to a broader lineshape of the $a_0(980)$ resonance compared to other processes.

Figure 6 (middle) displays the $\bar{K}^0\eta$ mass distribution, where a characteristic double-hump structure appears. The $K_0^*(1430)$ resonance contributes a peak at $M_{\bar{K}^0\eta} = M_{K_0^*} = 1425$ MeV with a width of $\Gamma_{K_0^*} = 270$ MeV, as given in Eq. (17). As discussed in the detail in Ref. [3], the interference between the $K_0^*(1430)$ and $a_0(980)$ components is responsible for the double-hump shape, requiring the phase ϕ in Table I to be negative.

Figure 6 (right) shows the $\bar{K}^0\pi^+$ mass distribution, which lacks a distinct peak but exhibits a broad bump around 1.25 GeV. Additionally, a discontinuity is visible at approximately 1.05 GeV. As discussed in the detail in Ref. [3], this feature results from applying a cut-off mass M_{cut} to the $G \cdot t$ terms in Eq. (15),

$$Gt(M_{\text{inv}}) = Gt(M_{\text{cut}}) e^{-\alpha(M_{\text{inv}} - M_{\text{cut}})} \quad (29)$$

following the approach outlined in Refs. [5, 33] to avoid going outside the range of validity of the chiral unitary approach. In this study, we use $M_{\text{cut}} = 1050$ MeV and $\alpha = 0.0037 \text{ MeV}^{-1}$.

B. Evaluation of a , r_0

In this part, we address the issue of evaluating the scattering length and effective range, not addressed in Ref. [3], which is the main purpose of the work. First we show the results for a and r_0 using the chiral unitary approach, with the potentials employed, following Refs. [34, 35] with $f = 93$ MeV as described before. The results are shown in Table II. These values are consistent with those of Ref. [36].

TABLE II: The value of a and r_0 [units in fm].

| $a_{K+\bar{K}}$ | $r_{0,K+\bar{K}}$ |
|--------------------|--------------------|
| $-0.124 - i 0.741$ | $-0.782 - i 0.182$ |

C. Resampling for a and r_0 with uncertainties

To estimate uncertainties in a and r_0 , we employ a resampling approach [21, 22, 37], fitting the parameters of the theory to data with Gaussian randomly distributed centroids of the points, with the same error. The procedure follows these steps: all terms in the interaction kernel V_{ij} from Refs. [34, 35] are proportional to $\frac{1}{f^2}$, where f is the pion decay constant. In Ref. [38], $f = 93$ MeV was used. Here, to allow flexibility in the potential and perform a model-independent analysis, we introduce the following modifications:

$$f \rightarrow f_{\pi\eta}, \quad \text{in the } \pi\eta \text{ channel;}$$

$$f \rightarrow f_{K\bar{K}}, \quad \text{in the } K\bar{K} \text{ channel.}$$

Then we obtain the different V -matrix of the coupled channels $K^+\bar{K}^0(1)$ and $\pi^+\eta(2)$

$$V_{11} = -\frac{s}{4f_{K\bar{K}}^2}, \quad V_{12} = -\frac{3s - m_{K^+}^2 - m_{\bar{K}^0}^2 - m_\eta^2}{3\sqrt{3}f_{K\bar{K}}f_{\pi\eta}},$$

$$V_{22} = -\frac{2m_\pi^2}{3f_{\pi\eta}^2}. \quad (30)$$

Now, we have 6 parameters C , D , ϕ , $f_{K\bar{K}}$, $f_{\pi\eta}$, q_{\max} where the values of f_i are sampled within the range $[40, 180]$ MeV. Additionally, we adjust the cutoff parameter, sampling q_{\max} within the range $[400, 1500]$ MeV. The resulting values of C , D , ϕ , f_i , $a_{K^+\bar{K}^0}$, $r_{0,K^+\bar{K}^0}$, and q_{\max} are presented in Table III. Using these parameters, we plot the different mass distributions in Fig. 7. A comparison with the experimental data shows that our theoretical results are in agreement with the data.

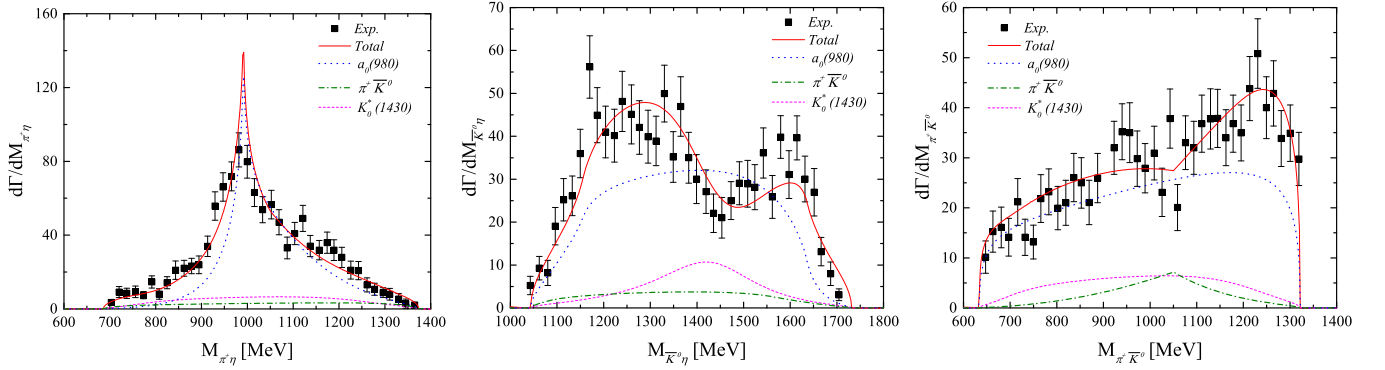


FIG. 7: After resampling: The mass distributions of $\pi^+\eta$ (left), $\bar{K}^0\eta$ (middle), and $\bar{K}^0\pi^+$ (right) with fixed $M_{\text{cut}} = 1050$ MeV. The parameters $C = 596.03$, $D = 49.86$, and $\phi = -1.85$ radians are used.

TABLE III: After resampling 100 times $\chi^2 = 2.25/d.o.f$ as a average for the different fits.

| C | D | ϕ [radians] |
|---------------------------------------|---------------------------------------|--------------------|
| 596.03 ± 29.92 | 49.86 ± 7.28 | -1.85 ± 0.64 |
| $f_{K^+\bar{K}^0}$ [MeV] | $f_{\pi\eta}$ [MeV] | q_{\max} [MeV] |
| 93.69 ± 5.88 | 92.96 ± 5.81 | 622.27 ± 39.31 |
| $a_{K^+\bar{K}^0}$ [fm] | $r_{0,K^+\bar{K}^0}$ [fm] | |
| $(-0.10 \pm 0.15) - i(0.70 \pm 0.14)$ | $(-0.81 \pm 0.15) - i(0.20 \pm 0.09)$ | |

These results indicate that $\text{Re}[a] \approx -0.10$ fm, while $\text{Im}[a] \approx -0.70$ fm, with uncertainties that are consistent with Table II. Similarly, $\text{Re}[r_0] \approx -0.81$ fm and $\text{Im}[r_0] \approx -0.20$ fm.

TABLE IV: Results for the $K^+\bar{K}^0$ scattering length from various studies.

| References | Ref. [12] | Ref. [13] | Ref. [39] | Ref. [40] | Ref. [11] |
|----------------|-------------------|-------------------|------------------|-------------------|---------------------------------------|
| $a(\text{fm})$ | $+0.071 - i 0.66$ | $-0.006 - i 0.76$ | $-0.13 - i 2.23$ | $-0.075 - i 0.70$ | $(-0.02 \pm 0.02) - i(0.63 \pm 0.24)$ |
| References | Ref. [13] | Ref. [41] | Ref. [14] | Ref. [15] | Ref. [36] |
| $a(\text{fm})$ | $-0.16 - i 1.05$ | $-0.13 - i 0.61$ | $-0.16 - i 0.59$ | $-0.54 - i 1.89$ | $-0.371 - i 0.549$ |

It is interesting to compare those results with other values obtained from different approaches and reactions for $a_{K^+\bar{K}^0}$, which we present in Table IV. As we can see, there is quite some dispersion in the values given by the different approaches. Our determination of $a_{K^+\bar{K}^0}$ provides also the uncertainty, and it is based on the analysis of a reaction with quite good statistics and a clean signal for the $a_0(980)$. In particular we would like to compare our results with those of [36], which were determined in

a similar way as done here, with a resampling analysis of the data of [42] for the $\chi_{c1} \rightarrow \eta\pi^+\pi^-$ reaction. The results obtained in [36] are

$$\begin{aligned} a_{K^+\bar{K}^0} &= -(0.371 \pm 0.045) - i(0.549 \pm 0.023), \\ r_{0,K^+\bar{K}^0} &= -(0.982 \pm 0.107) - i(0.265 \pm 0.035). \end{aligned} \quad (31)$$

We first see that the errors in Eq. (31) are smaller than those that we get here in Table III. This is understandable since the experimental errors in [42] are smaller than in the reaction studied here [2]. If we look at $\text{Re}(a_{K^+\bar{K}^0})$, playing with uncertainties, the results of [36] would provide a minimum value of -0.32 fm (minimum of the absolute value), while the maximum value here is -0.26 fm. They are not far away, and the difference is small when compared with the dispersion of values in Table IV. So, we can give a more precise value of $\text{Re}(a_{K^+\bar{K}^0})$ than can be anticipated from the values in Table IV. On the other hand $\text{Im}(a_{K^+\bar{K}^0}) = -(0.549 \pm 0.023)$ fm in [36] overlaps within errors with our value in Table III.

We take advantage to point out that the effective range was determined for the first time in [36] with the results of Eq. (31). One can see again that the results obtained in [36] and those obtained here for the effective range are perfectly compatible within errors. In summary, the results obtained here for $a_{K^+\bar{K}^0}$ provide a precise value for this magnitude, and those for the effective range, determined for the first time in [36] and here, offer also a precise determination of this magnitude.

IV. CONCLUSION

We investigate the $D^+ \rightarrow \bar{K}^0\pi^+\eta$ reaction with the purpose of obtaining a precise determination of the $K^+\bar{K}^0$ scattering parameters. Our study begins with a comprehensive analysis of the dominant weak decay mechanisms at the quark level, focusing on both external and internal emission contributions. We find that the external emission contributions vanish, providing a clearer understanding of the decay process. We use the chiral unitary approach, where the $a_0(980)$ resonance is generated by the interaction between the $\pi\eta$ and $K\bar{K}$ channels. This resonance plays a crucial role in shaping the mass distributions, especially in the $\pi^+\eta$ channel, where we observe a clear peak around 1.0 GeV, corresponding to this resonance.

Furthermore, our analysis obtained the same important features already discussed in Ref. [3]. These analysis reveals important features of the $\bar{K}^0\eta$ and $\bar{K}^0\pi^+$ mass distributions. The $\bar{K}^0\eta$ distribution exhibits a distinctive double-hump structure due to the interference between the $a_0(980)$ and $K_0^*(1430)$ resonances, with the phase ϕ playing a crucial role in determining the shape. On the other hand, the $\bar{K}^0\pi^+$ distribution is rather structureless.

In addition, we provide an evaluation of the $K^+\bar{K}^0$ scattering length (a) and effective range (r_0) using the chiral unitary approach, with values that align well with previous theoretical results. To estimate the uncertainties in these magnitudes, we used a resampling method, adjusting the parameters of the pion decay constant and the cut-off. The procedure rendered values of a and r_0 and, very importantly, their uncertainties. Together with the results of [36], these values provide the most accurate results at present.

In summary, our work not only provides a detailed understanding of the $D^+ \rightarrow \bar{K}^0\pi^+\eta$ reaction, but also enhances our knowledge of the underlying dynamics governing the scattering processes in the system. The sharp cusp near the $K^+\bar{K}^0$ threshold and the double-hump structure in the $\bar{K}^0\eta$ distribution provide important insights into the interactions between pseudoscalar meson, and the uncertainties in the parameters are well quantified using the resampling approach. The method, together with the results of [36], provide the most accurate results for a , r_0 of $K^+\bar{K}^0$ at present.

V. ACKNOWLEDGMENTS

We would like to sincerely thank Prof. Natsumi Ikeno for the careful revision of this manuscript. This work is partly supported by the National Natural Science Foundation of China under Grants No. 12405089 and No. 12247108 and the China Postdoctoral Science Foundation under Grant No. 2022M720360 and No. 2022M720359. ZY.Yang and J. Song wish to thank support from the China Scholarship Council. This work is also supported by the Spanish Ministerio de Economía y Competitividad (MINECO) and European FEDER funds under Contracts No. FIS2017-84038-C2-1-P B, PID2020- 112777GB-I00, and by Generalitat Valenciana under contract PROMETEO/2020/023. This project has received funding from the European Union Horizon 2020 research and innovation programme under the program H2020- INFRAIA-2018-1, grant agreement No. 824093 of the STRONG-2020 project. This work is supported by the Spanish Ministerio de Ciencia e Innovación (MICINN) under contracts PID2020-112777GB-I00, PID2023-147458NB-C21 and CEX2023-001292-S; by Generalitat Valenciana under contracts PROMETEO/2020/023 and CIPROM/2023/59. This work is partly supported by the National Natural Science Foundation of China (NSFC) under Grants No. 12365019 and No. 11975083, and by the Central Government Guidance Funds for Local Scientific and Technological Development, China (No. Guike ZY22096024), the Natural Science Foundation of Guangxi

province under Grant No. 2023JJA110076.

-
- [1] M. Ablikim et al. (BESIII), Phys. Rev. Lett. **124**, 241803 (2020).
 - [2] M. Ablikim et al. (BESIII), Phys. Rev. Lett. **132**, 131903 (2024).
 - [3] N. Ikeno, J. M. Dias, W.-H. Liang, and E. Oset, Eur. Phys. J. C **84**, 469 (2024).
 - [4] Y. Q. Chen et al. (Belle), Phys. Rev. D **102**, 012002 (2020).
 - [5] G. Toledo, N. Ikeno, and E. Oset, Eur. Phys. J. C **81**, 268 (2021).
 - [6] J. A. Oller and E. Oset, Nucl. Phys. A **620**, 438 (1997), [Erratum: Nucl.Phys.A 652, 407–409 (1999)].
 - [7] N. Kaiser, Eur. Phys. J. A **3**, 307 (1998).
 - [8] F.-K. Guo, C. Hanhart, U.-G. Meißner, Q. Wang, Q. Zhao, and B.-S. Zou, Rev. Mod. Phys. **90**, 015004 (2018), [Erratum: Rev.Mod.Phys. 94, 029901 (2022)].
 - [9] S. M. Flatte, Phys. Lett. B **63**, 224 (1976).
 - [10] N. N. Achasov and V. N. Ivanchenko, Nucl. Phys. B **315**, 465 (1989).
 - [11] M. Buescher, A. Dzyuba, V. Kleber, S. Krewald, R. H. Lemmer, and F. P. Sassen, Phys. Lett. B **633**, 265 (2006).
 - [12] A. Aloisio et al. (KLOE), Phys. Lett. B **536**, 209 (2002).
 - [13] N. N. Achasov and A. V. Kiselev, Phys. Rev. D **68**, 014006 (2003).
 - [14] S. Teige et al. (E852), Phys. Rev. D **59**, 012001 (1999).
 - [15] M. Bargiotti et al. (OBELIX), Eur. Phys. J. C **26**, 371 (2003).
 - [16] G. Colangelo, J. Gasser, B. Kubis, and A. Rusetsky, Phys. Lett. B **638**, 187 (2006).
 - [17] J. R. Batley et al., Eur. Phys. J. C **64**, 589 (2009).
 - [18] S. B. Yang et al. (Belle), Phys. Rev. D **108**, L031104 (2023).
 - [19] M.-Y. Duan, M. Bayar, and E. Oset, Phys. Lett. B **857**, 139003 (2024).
 - [20] J. A. Oller, E. Oset, and A. Ramos, Prog. Part. Nucl. Phys. **45**, 157 (2000).
 - [21] M. Albaladejo, D. Jido, J. Nieves, and E. Oset, Eur. Phys. J. C **76**, 300 (2016).
 - [22] B. Efron and R. Tibshirani, Statist. Sci. **57**, 54 (1986).
 - [23] J. D. Weinstein and N. Isgur, Phys. Rev. Lett. **48**, 659 (1982).
 - [24] V. Baru, J. Haidenbauer, C. Hanhart, Y. Kalashnikova, and A. E. Kudryavtsev, Phys. Lett. B **586**, 53 (2004).
 - [25] T. Hyodo and M. Niiyama, Prog. Part. Nucl. Phys. **120**, 103868 (2021).
 - [26] A. Bramon, A. Grau, and G. Pancheri, Phys. Lett. B **283**, 416 (1992).
 - [27] X.-L. Ren, E. Oset, L. Alvarez-Ruso, and M. J. Vicente Vacas, Phys. Rev. C **91**, 045201 (2015).
 - [28] J. Gasser and H. Leutwyler, Annals Phys. **158**, 142 (1984).
 - [29] S. Scherer, Adv. Nucl. Phys. **27**, 277 (2003).
 - [30] S. Navas et al. (Particle Data Group), Phys. Rev. D **110**, 030001 (2024).
 - [31] J.-X. Lin, J.-T. Li, S.-J. Jiang, W.-H. Liang, and E. Oset, Eur. Phys. J. C **81**, 1017 (2021).
 - [32] N. Ikeno, G. Toledo, and E. Oset, Phys. Lett. B **847**, 138281 (2023).
 - [33] V. R. Debastiani, W.-H. Liang, J.-J. Xie, and E. Oset, Phys. Lett. B **766**, 59 (2017).
 - [34] W. H. Liang and E. Oset, Phys. Lett. B **737**, 70 (2014).
 - [35] J.-J. Xie, L.-R. Dai, and E. Oset, Phys. Lett. B **742**, 363 (2015).
 - [36] H.-P. Li, J.-X. Lin, W.-H. Liang, and E. Oset (2024), 2409.16696.
 - [37] W. H. Press, S. A. Teukolsky, W. T. Vetterling, and B. P. Flannery (1992).
 - [38] W.-H. Liang, J.-J. Xie, and E. Oset, Eur. Phys. J. C **76**, 700 (2016).
 - [39] M. N. Achasov et al., Phys. Lett. B **479**, 53 (2000).
 - [40] D. V. Bugg, V. V. Anisovich, A. Sarantsev, and B. S. Zou, Phys. Rev. D **50**, 4412 (1994).
 - [41] A. Abele et al., Phys. Rev. D **57**, 3860 (1998).
 - [42] M. Ablikim et al. (BESIII), Phys. Rev. D **95**, 032002 (2017).